Improving low-resolution gas-mixture absorption spectra using neural networks

Skiba V.E.[1], Vrazhnov D.A.[1,2], Prischepa V.V.[1], Miroshnichenko M.B.[2]

[1]National Research Tomsk State University, Tomsk, Russia
[2]Institute of Strength Physics and Materials Science of SB RAS, Tomsk, Russia

ABSTRACT

An important role in component analysis with spectral methods has a spectral resolution of used tools. The most useful and perspective methods to improve spectral resolution is decreasing of impulse response function (IRF) and improving resolution using superresolution (SR) reconstruction methods. We have analyzed different types of neural networks (convolution neural network, multilayered perceptron) for improving the spectral resolution of initial absorption spectra. The used approach is based on an association of a high-resolution and a low-resolution spectrum. The latter was constructed from high-resolution spectra to which IRF and some random noise were added. High-resolution spectra were generated using the HITRAN database. Most optimal architectures of neural networks to improve spectral resolution were defined.

Keywords: absorption spectra, neural network, multilayered perceptron, convolutional neural network, super-resolution reconstruction, Pearson criterion

1. INTRODUCTION

Superresolution is a method, which allows recovering a high-resolution (HR) image from a low-resolution (LR) one. In general, low-resolution images I_x can be modelled as output of the following degradation function [1]:

$$I_x = D(I_y;\ \delta) \tag{1}$$

where D denotes degradation mapping function, I_y – HR image, δ – degradation parameters, such as scaling coefficient, noises, impulse response functions of equipment [2] and others. Generally, degradation function (e.g., D and δ) are unknown, and only LR images are provided. Also, in degradation function can be various nonlinear parameters such as compression artifacts, anisotropic degradations. For model developing, researchers use downsampling operations as degradation function:

$$D(I_y;\ \delta) = (I_y)\downarrow_s \{S\} \subset \delta \tag{2}$$

where $\downarrow_s$ is downsampling operation with some scaling factor S., most datasets for generic SR are built based on this pattern, and the most commonly used downsampling operation is bicubic interpolation with antialiasing. However, there are other works [3] modeling degradation as a combination of several operations:

$$D(I_y;\ \delta) = (I_y\ \otimes k)\downarrow_s + n_\varsigma\{k, s, \varsigma\} \subset \delta \tag{2}$$

where $(I_y\ \otimes k)$ represents the convolution between a blur kernel k and the HR image I_y, and n_ς is some additive white Gaussian noise with standard deviation ς.

In general, the SR reconstruction approach has a wide range of real-world applications such as medical imaging [4], [5], [6], surveillance, security [7], [8], lases spectroscopy [9][10] and others.

In this paper, several artificial neural network (ANN) architectures have been tested and compared, such as multilayer perceptron and convolutional neural networks for a gas mixture absorption spectra SR reconstruction.

2. ANN TRAINING AND TESTING DATA GENERATION

For ANN training and testing, a dataset of high-resolution spectra with different values of concentrations for various components was generated using the HITRAN database [11]. We used gas mixtures of C_2H_2, CS, CO, HI, HC_1, H_2O, NH_3, O_3. Generated absorption spectra were limited by the following conditions:

1. Wavenumber range from 900 cm^{-1} to 7400 cm^{-1} ($0{,}9091 - 7{,}4\ \mu m$);
2. Temperature T = 296 K;
3. Pressure P = 1 atm;
4. Profile: Voigt;
5. Wing: 50 HW;
6. Scut: $1e^{-28}$ cm/mol

Concentrations were randomized for creating a gas mixes dataset. An example of the generated absorption spectrum of a gas mixture is shown in Figure 1.

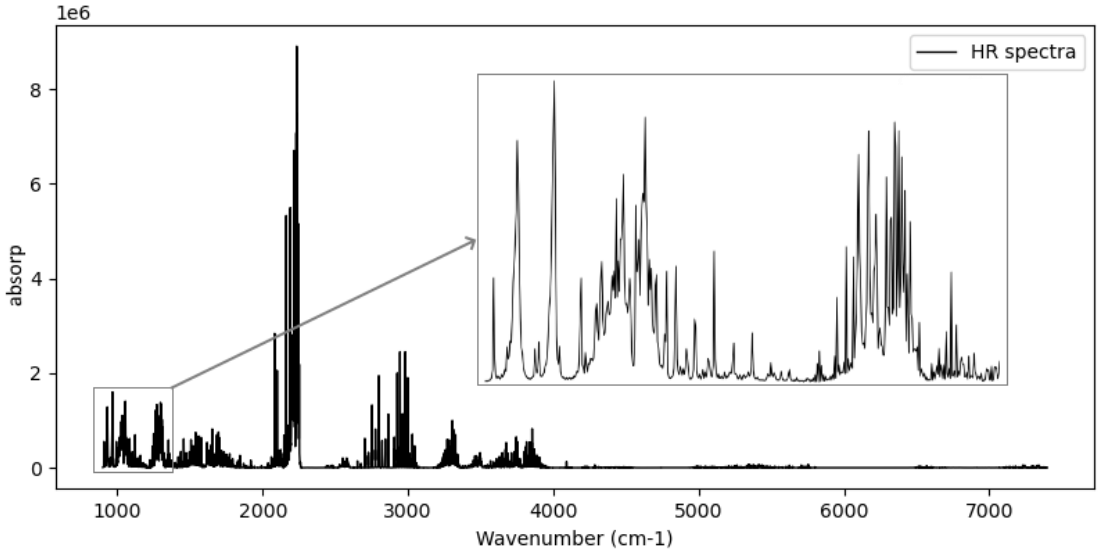

Figure 1 – Generated high-resolution spectrum

For generating training and testing datasets with HR spectra and LR spectra, HR spectra were processed with a degradation function. We used a Gaussian filter:

$$G(x) = \frac{1}{\sqrt{2\pi\sigma}} e^{-\frac{x^2}{2\sigma^2}} \tag{3}$$

where σ is the standard deviation. The result of the high-resolution spectrum transformation with the Gaussian filter is shown in Figure 2.

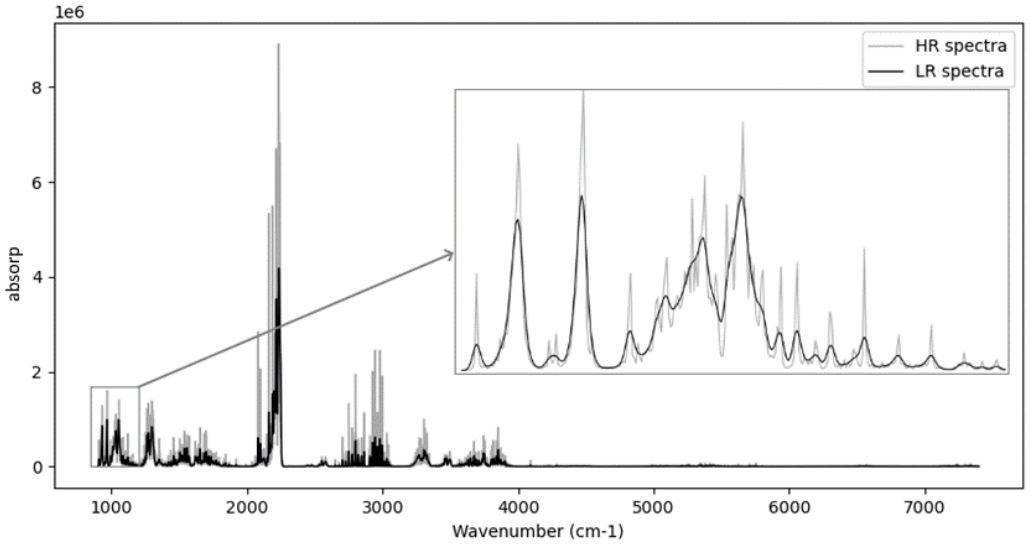

Figure 2 – Generated low-resolution spectrum

3. NETWORKS ARCHITECTURE

Multilayered perceptron (MLP) and convolutional neural network architectures were chosen for simulation. The developed MLP-architecture was shown in Figure 3.

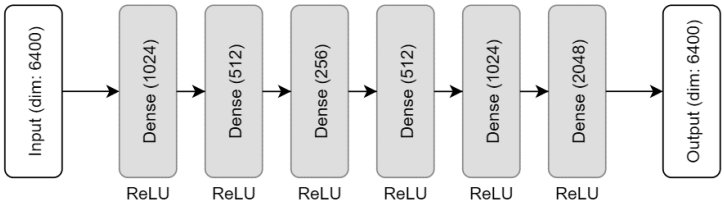

Figure 3 – MLP architecture

The MLP input and output vector dimensions are the same to construct an association between a LR and a HR spectrum. Six hidden layers with the ReLU activation function were used [12].

Autoencoder architecture based on deep convolutional neural networks (DCNN) is often used for solving audio-signal [13], [14], and image SR problems, so such architecture was chosen for testing and comparing. For comparing two different implementations of autoencoder based on DCNN was developed. The difference is that the second neural network use cross-connections and various types of layers. The architecture of the first network (CNN1) is shown in Figure 4.

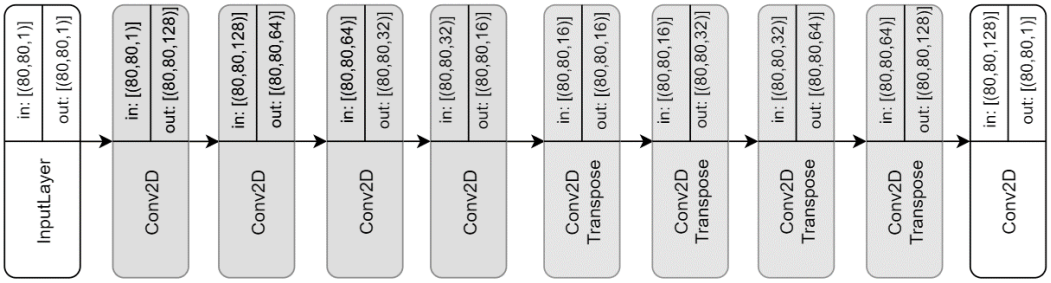

Figure 4 – CNN1 architecture

In this network, Conv2D and Conv2DTransposed layers were used. These layers work with 2-dimensional input data, so the input vector for 6400 elements was reshaped to 80x80 matrix, which was reshaped to a single-dimensional vector again after the neural network is finished its work. The ReLU activation function was used for all layers.

The second convolutional neural network was built using autoencoder architecture too, but it used MaxPooling2D layer and UpSampling2D layer, which helps to determine and pick most important data for each step. Also, these layers are used for downsampling (MaxPooling2D) and the next upsampling (UpSampling2D) of input data.

The second convolutional neural network (CNN2) architecture is shown in Figure 5.

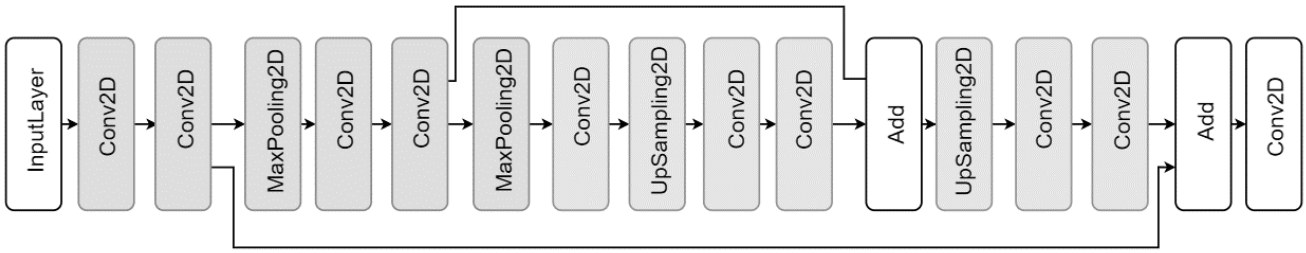

Figure 5 – CNN2 architecture

4. NETWORKS TRAINING AND TESTING

For network training and testing, the dataset for 10000 absorption spectra was generated using described above components with various concentrations. Then 10000 high-resolution spectra were transformed into low-resolution ones.

Network learning quality was tested on three different variants of training and testing sets ratio (70% / 30%, 80% / 20%, 60% / 40%).

The result of the work learned MLP (70x30) is shown in Figure 6.

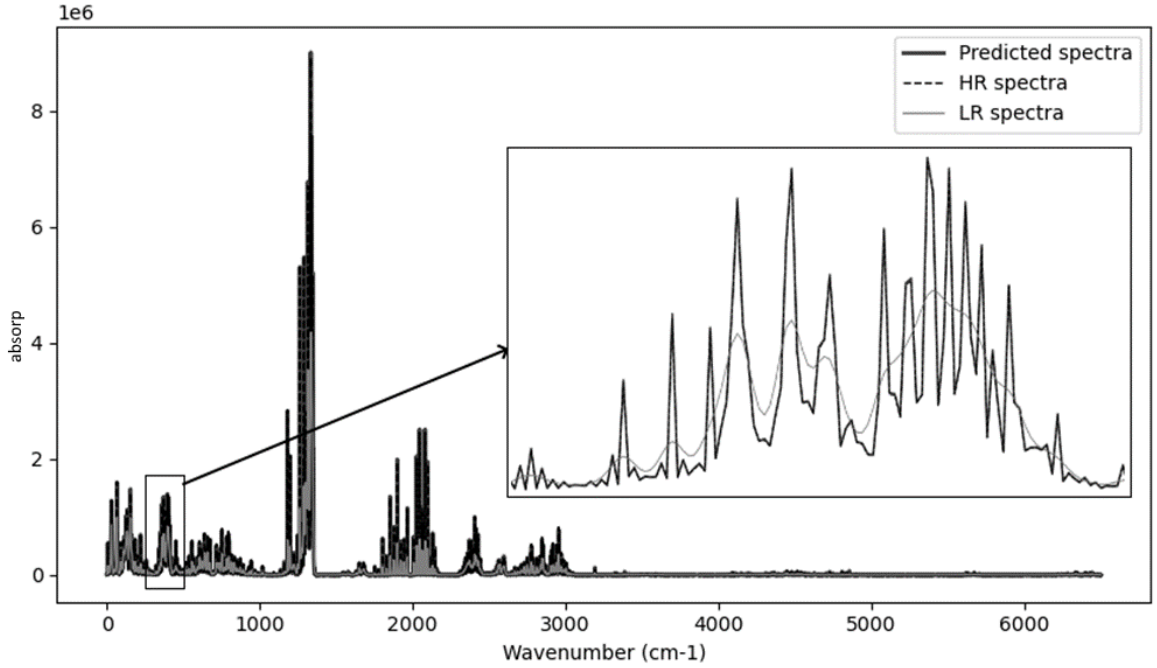

Figure 6 – Result of MLP application for spectrum resolution reconstruction

For spectrum resolution quality estimation, a Pearson-like correlation coefficient was used [15]. This coefficient shows how predicted by the neural network spectrum is close to the HR spectrum. The formula for the Pearson-like correlation coefficient is as follows:

$$S = \frac{\sum_i |X_i - Y_i|}{\frac{1}{2}\sum_i |X_i + Y_i|} \quad (4)$$

where X_i, Y_i – absorption coefficients of compared spectra at the same wavenumber. It's important to note that the dimension of the compared spectra must be the same. The calculated Pearson-like correlation coefficient was converted to a percentage scale, to show the efficiency of ANN work and shown in Table 1.

Table 1 – Comparison of neural networks efficiency

	Min (%)	Max (%)	Average (%)
Spectra split 70% by 30%			
MLP	**84,5**	**97,34**	**95,14**
CNN1	39	83,86	75,47
CNN2	64,57	91,35	87,78
Spectra split 80% by 20%			
MLP	**84,64**	**97,71**	**95,36**
CNN1	34,62	87,3	79,84
CNN2	67,22	91,18	87,87
Spectra split 60% by 40%			
MLPa	**84,23**	**96,11**	**94,24**
CNN1	33,45	81,25	73,2
CNN2	64,4	90,89	87,45

Distribution graph, which shows how the percentage of efficiency is distributed by testing dataset (1650 spectra) is shown below:

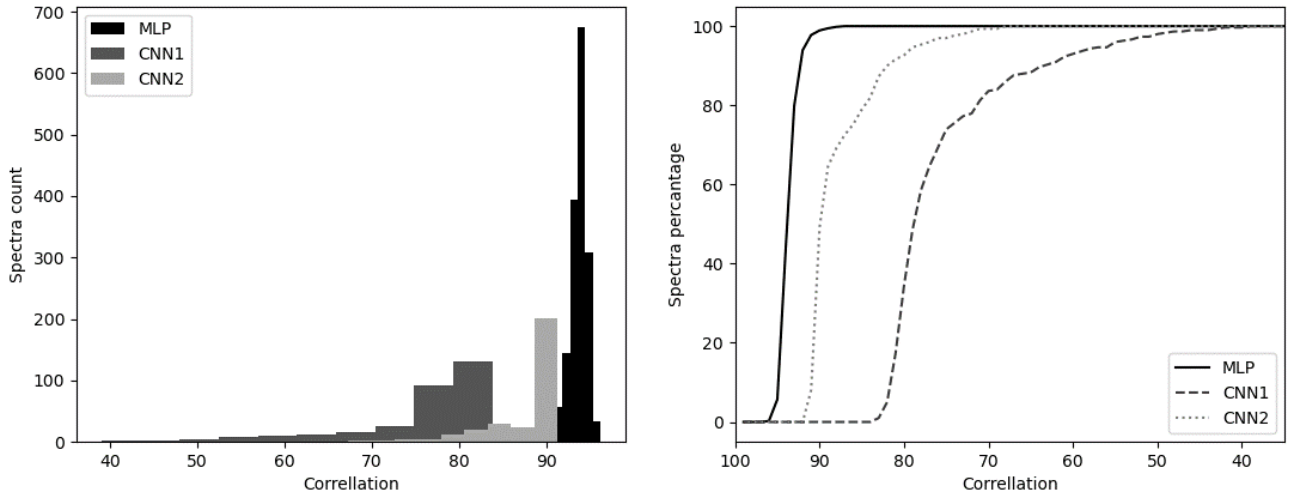

Figure 7 – Neural network application efficiency distribution

On the left side of figure 7, the distribution of correlation between HR spectra and neural network prediction results is shown, the distribution of the percentage of efficiency is on the right side. We can see that for the MLP network, 98% of spectra is recovered for 95% efficiency.

5. CONCLUSION

The presented results show that a spectrum resolution improving quality using ANN is good enough. CNN, which uses only on Conv2D layers, provides the average correlation coefficient of about 75%. CNN, which uses MaxPooling2D and UpSampling2D, provides the average correlation coefficient of about 87%. The best result (95%) has been obtained using MLP. The correlation coefficient distribution has a nonsymmetric shape with a right-shifted maximum. It shows that there are fewer bad recovery results than good ones.

ACKNOWLEDGMENTS

The work was carried out under partial financial support of the Russian Fund of Basic Research (grant No.17-00-00186). The work was performed under the government statement of work for ISPMS Project No. III.23.2.10.

REFERENCES

[1] Z. Wang, J. Chen and S. C. H. Hoi, "Deep Learning for Image Super-resolution: A Survey," in IEEE Transactions on Pattern Analysis and Machine Intelligence, doi: 10.1109/TPAMI.2020.2982166.

[2] Kolker D.B., Pustovalova, R.V., Starikova, M.K., Kuznetsov, O.M., Kistenev, Y.V., Optical parametric oscillator within 2.4–4.3 μm pumped with a nanosecond Nd:YAG Laser, Atmospheric and Oceanic Optics 25(1), c. 77-81, 2012

[3] K. Zhang, W. Zuo, and L. Zhang, "Learning a single convolutional superresolution network for multiple degradations," in CVPR, 2018.

[4] H. Greenspan, "Super-resolution in medical imaging," The Computer Journal, vol. 52, 2008.

[5] J. S. Isaac and R. Kulkarni, "Super resolution techniques for medical image processing," in ICTSD, 2015.

[6] Y. Huang, L. Shao, and A. F. Frangi, "Simultaneous superresolution and cross-modality synthesis of 3d medical images using weakly-supervised joint convolutional sparse coding," in CVPR, 2017.

[7] L. Zhang, H. Zhang, H. Shen, and P. Li, "A superresolution reconstruction algorithm for surveillance images," Elsevier Signal Processing, vol. 90, 2010.

[8] P. Rasti, T. Uiboupin, S. Escalera, and G. Anbarjafari, "Convolutional neural network super resolution for face recognition in surveillance monitoring," in AMDO, 2016.

[9] Kistenev Y.V., Bukreeva E.B., Bulanova A.A., Tuzikov S.A., Yumov E.L., Laser spectroscopy and chemometric study of the specific features of air exhaled by patients with lung cancer and chronic obstructive pulmonary disease, Physics of Wave Phenomena 22(3), c. 210-215, 2014.

[10] Kistenev, Y.V., Kuzmin, D.A., Vrazhnov, D.A., Borisov, A.V., Classification of patients with broncho-pulmonary diseases based on analysis of absorption spectra of exhaled air samples with SVM and neural network algorithm application, Proceedings of SPIE - The International Society for Optical Engineering 10035,1003507, 2016.

[11] Kistenev, Y.V., Shapovalov, A.V., Borisov, A.V., Nikolaev, V.V., Nikiforova, O.Y., Applications of principal component analysis to breath air absorption spectra profiles classification, Proceedings of SPIE - The International Society for Optical Engineering 9810,98101Y, 2015.

[12] Abien Fred M. Agarap, Deep Learning using Rectified Linear Units (ReLU), arXiv:1803.08375v2 [cs.NE] 7 Feb 2019

[13] Kuleshov V., Enam S. Z., Ermon S. Audio superresolution using neural nets //ICLR (Workshop Track). – 2017

[14] Lim T. Y. et al. Time-frequency networks for audio superresolution //2018 IEEE International Conference on Acoustics, Speech and Signal Processing (ICASSP). – IEEE, 2018. – C. 646-650

[15] *Greenwood P.E., Nikulin M.S.*, [A guide to chi-squared testing] John Wiley and Sons, New York, 280 (1996)